REVIEW

Decoding the mechanisms of gait generation in salamanders by combining neurobiology, modeling and robotics

**Andrej Bicanski · Dimitri Ryczko · Jérémie Knuesel · Nalin Harischandra ·
Vanessa Charrier · Örjan Ekeberg · Jean-Marie Cabelguen · Auke Jan Ijspeert**

Abstract Vertebrate animals exhibit impressive locomotor skills. These locomotor skills are due to the complex interactions between the environment, the musculo-skeletal system and the central nervous system, in particular the spinal locomotor circuits. We are interested in decoding these interactions in the salamander, a key animal from an evolutionary point of view. It exhibits both swimming and stepping gaits and is faced with the problem of producing efficient propulsive forces using the same musculo-skeletal system in two environments with significant physical differences in density, viscosity and gravitational load. Yet its nervous system remains comparatively simple. Our approach is based on a combination of neurophysiological experiments, numerical modeling at different levels of abstraction, and robotic validation using an amphibious salamander-like robot. This article reviews the current state of our knowledge on salamander locomotion control, and presents how our approach has allowed us to obtain a first conceptual model of the salamander spinal locomotor networks. The model suggests that the salamander locomotor circuit can be seen as a lamprey-like circuit controlling axial movements of the trunk and tail, extended by specialized oscillatory centers controlling limb movements. The interplay between the two types of circuits determines the mode of locomotion under the influence of sensory feedback and descending drive, with stepping gaits at low drive, and swimming at high drive.

A. Bicanski (✉) · J. Knuesel · A. J. Ijspeert
Biorobotics Laboratory, School of Engineering,
École Polytechnique Fédérale de Lausanne, Station 14,
1015 Lausanne, Vaud, Switzerland
e-mail: andrej.bicanski@epfl.ch
http://biorob.epfl.ch

D. Ryczko
Groupe de Recherche sur le Système Nerveux Central,
Département de Physiologie, Université de Montréal, Montréal,
QC H3C 3J7, Canada

N. Harischandra
Department of Computational Biology, KTH Royal Institute of
Technology, School of Computer Science and Engineering,
Stockholm, Sweden

N. Harischandra
Department of Biological Cybernetics, Faculty of Biology,
University of Bielefeld, Bielefeld, Germany

V. Charrier · J.-M. Cabelguen
INSERM U862, Neurocentre Magendie,
Motor System Diseases Group, Université Bordeaux,
146 rue Leo Saignat, 33077 Bordeaux Cedex, France

Ö. Ekeberg
Department of Computational Biology, KTH Royal Institute of
Technology, School of Computer Science and Communication,
Stockholm, Sweden

1 Introduction

Among vertebrates, salamanders constitute a group that is particularly well-suited to investigate how tetrapods adapt their locomotion to explore different environments. As amphibians, they are capable of displaying a variety of aquatic and terrestrial locomotor gaits.

In water, salamanders are capable of swimming and forward stepping. The swimming gait, which is the fastest gait of the salamander, is similar to that of the lamprey with axial undulations being propagated as traveling waves

from the head to the tail ("anguilliform swimming") (Frolich and Biewener 1992; D'Août et al. 1996; Gillis 1997). During forward underwater stepping, salamanders use either standing or head-to-tail traveling waves of axial undulation (Ashley-Ross et al. 2009; Deban and Schilling 2009; Lamarque et al. 2009). During forward stepping on firm ground, combinations of standing and travelling mechanical waves have been reported, depending on the speed of locomotion or type of stepping gait.[1] In our own recordings (Delvolvé et al. 1997) we mainly observed standing waves (for a detailed analysis of salamander kinematics during forward land stepping, forward underwater stepping, and swimming, see Karakasiliotis et al. 2012 in the same issue).

During swimming, the limbs are folded backwards along the side of the body whereas during underwater or land stepping they move rhythmically (Frolich and Biewener 1992; Ashley-Ross 1994a; Delvolvé et al. 1997; Ashley-Ross et al. 2009). Periods of suspension (i.e., with no limbs in contact with the substrate) are more often observed during underwater stepping due to the substantial buoyancy in water (Ashley-Ross et al. 2009).

In addition to these typical swimming and stepping gaits, salamanders can use some specialized forms of locomotion, which have not been investigated systematically because of the difficulties to elicit them. Salamanders sometimes use crawling as a second terrestrial gait, for instance when trying to rapidly escape in grass. This crawling gait is very similar to swimming movements on ground (i.e., with limbs folded against the body) (Ashley-Ross 1994a,b; Edwards 1977). In water, salamanders can sometimes exhibit low-speed paddling with the limbs, associated with small axial rhythmic movements (Frolich and Biewener 1992; Ashley-Ross 1994a,b; Delvolvé et al. 1997). Salamanders can spontaneously exhibit short episodes of backward stepping during manoeuvring on land. Thereafter, to reach the desired location, they quickly switch to forward stepping, which is a more efficient locomotor mode. Much longer episodes of backward stepping can be induced by training the animal to walk backward on a motorized treadmill (Ashley-Ross and Lauder 1997). To the best of our knowledge there is so far no report of backward swimming in salamanders, although caudorostral waves of motoneuron activity (i.e., negative phase lags) have been observed in vitro in the axial spinal cord of *Pleurodeles*

---

[1] Henceforth the following distinctions are made between locomotor modes (e.g., swimming vs. stepping) and between gaits. The locomotor mode of stepping encompasses (i) at slow speeds, a sequential walking gait, where one foot is lifted off the ground at a time. The order in which the feet are lifted defines the further subdivision in lateral sequence walk (ipsilateral hindlimb follows the ipsilateral forelimb) and diagonal sequence walk (contralateral hindlimb follows the ipsilateral forelimb). (ii) At higher speeds, a walking trot gait, where diagonally opposite feet are lifted roughly simultaneously off the ground. At even higher speeds the walking trot turns into a running trot, with short flight phases (Daan and Belterman 1968; Carrier 1993; Ashley-Ross 1994a).

waltlii (Delvolvé et al. 1999). However, tail to head propagated waves of axial muscle contractions have been reported during struggling movements induced by grasping the pelvic girdle during ongoing overground stepping in salamanders (Lamarque et al. 2009).

Locomotor movements emerge from complex dynamic interactions between the central nervous system, the peripheral sensory inputs, the musculo-skeletal system, and the environment (Pearson et al. 2006). The complexity of these interactions is high in amphibians because these animals are faced with the problem of efficiently producing propulsive forces using the same musculo-skeletal system in two environments with physical disparities (e.g., in terms of density, viscosity, and gravitational load).

A promising approach to fully understand locomotor systems is to combine neurobiology, neuro-mechanical modeling with bio-inspired robotics (Ijspeert 2001; Ijspeert et al. 2007). Indeed, it is now clear that these dynamic systems cannot be properly understood only by neurobiological investigations (e.g., "circuit cracking"). The goal of this paper is to illustrate how this inter-disciplinary approach has been fruitful to decode the mechanisms underlying gait generation and gait transition in salamanders.

2 Organization of the locomotor CPG in salamanders

During locomotion in vertebrates, the rhythmic and coordinated activations of axial and limb muscles are generated by neural networks called central pattern generators (CPGs) (Grillner 1981), which are located in the spinal cord. It is convenient to distinguish the networks controlling trunk and tail motions, i.e., the axial locomotor CPG, from those controlling limb motions, i.e. the limb CPG (Ijspeert 2008).

A central idea that has been used to build a model of the architecture of the salamander CPG is that the network controlling axial motion may have been inherited from older, swimming vertebrates, like the lamprey (Edwards 1977; Grillner and Wallén 1985; Cohen et al. 1988; Delvolvé et al. 1997; Ijspeert 2001). This conserved swimming circuitry would have been phylogenetically extended by the addition of new networks controlling the limbs. At the behavioral level, this hypothesis is consistent with the observation that salamanders and lampreys share the same anguilliform swimming mode (for neural network homologies between lamprey and salamander, see Ryczko et al. 2010b). Note that in evolutionary more distant organisms, convergent evolution may play a stronger role than conservation of neural circuits (Mullins et al. 2011). Similarly to adult lampreys (Wallén and Williams 1984), the isolated spinal cord of adult salamanders generates waves of ventral root activity that alternates between left and right sides and propagates along the spinal

cord when chemically activated with N-methyl-D-aspartate (NMDA) (Delvolvé et al. 1999; Ryczko et al. 2010a). In both species, the intersegmental phase lags range from positive values (i.e., rostrocaudal waves) to negative values (i.e., caudorostral waves) (Matsushima and Grillner 1992; Ryczko et al. 2009). The diversity of phase lags has been related to the diversity of gaits observed in vivo in both species (Matsushima and Grillner 1992; Lamarque et al. 2009; Ryczko et al. 2009).

In the lamprey three different coupling mechanisms between ipsilateral oscillators have been proposed for generating the intersegmental phase lags: (a) balanced descending and ascending coupling (Matsushima and Grillner 1992). This hypothesis is based on the in vitro demonstration that a leading rostral or caudal oscillator can entrain the rest of the cord with similar effects on cycle duration and intersegmental phase lag ("trailing oscillator" hypothesis). A leading oscillator receives stronger drive and thus has a higher intrinsic frequency; (b) dominant descending coupling (Hagevik and McClellan 1994). This mechanism relies on experiments showing that pharmacological disruption of the left–right alternation in the rostral spinal cord also disrupted alternation in some segments located caudally, whereas pharmacological disruption of alternation in the caudal spinal cord had weaker disruptive effects on the segments located more rostrally. Several other experimental and modeling studies support the notion of dominantly descending coupling in the lamprey spinal cord. Buchanan and co-workers have shown that intersegmental connections of both excitatory and inhibitory commissural inter-neurons are dominantly caudally directed (Buchanan et al. 1989; Buchanan 2001). Kozlov and collaborators have used these couplings in biologically detailed modeling studies on the lamprey spinal cord (Kozlov et al. 2007, 2009); (c) dominant ascending coupling (Williams et al. 1990; Cohen et al. 1992; Kopell et al. 1991). This mechanism was based on the observation that rhythmic bending of the caudal end (but not the rostral end) of the spinal cord can entrain the spinal cord to generate a rhythm below the "natural frequency" of the cord (Williams et al. 1990). However, in this study coupling dominance was defined in abstract mathematical terms rather than relating directly to physiological properties.

Models based on these three mechanisms can generate the rostrocaudal phase lags observed during swimming in the lamprey (see also Ijspeert et al. 2005). Biological data heterogeneously supports these three mechanisms. In invertebrates, models with asymmetries in the couplings between the segmental oscillators were also used to explain the longitudinal coordination during swimming in the leech or in the crayfish swimmeret (for review, see Hill et al. 2003). In the salamander the neuronal mechanisms underlying the variability of the patterns generated by the axial CPG are not fully understood. However, several biological and modeling studies suggest that the descending inputs and movement-related sensory inputs could play a critical role.

2.1 The trunk networks

At the segmental level, our recent experiments provide direct evidence of a strong similarity of the global architecture of the axial locomotor CPG of the salamander at the level of the trunk (Ryczko et al. 2010a) with that of the swimming CPG of the lamprey (for review, see Grillner 2006). Surgically isolated segments and hemisegments from the mid-trunk spinal cord of adult salamanders are able to generate a rhythmic activity when pharmacologically activated. The salamander axial CPG consists of a double chain of identical oscillators (pools of neurons that produce a rhythmic activity) that are coupled by reciprocal inhibition to produce left-right alternation. Reciprocal excitatory connections were also revealed by pharmacologically blocking reciprocal inhibition (Ryczko et al. 2010a), but the function of these connections is unclear. Our previous modeling studies of the axial circuitry based on various levels of abstraction (Ijspeert 2001; Bem et al. 2003; Ijspeert et al. 2007) also support the idea of a double chain of oscillators, as in the lamprey CPG (Cangiano and Grillner 2003). However, some differences between salamanders and lampreys as to the intrinsic neuronal properties underlying the bursting of spinal segments have been observed. For example, blocking apamine-sensitive calcium-activated potassium channels does not disrupt the regularity of locomotor bursts in isolated salamander segments/hemisegments (Ryczko et al. 2010a), whereas it can disrupt, or even abolish the regularity of the locomotor bursts elicited by a low concentration of NMDA in the lamprey spinal cord (El Manira et al. 1994).

Based on these new findings, we have recently proposed a tentative model of axial spinal segments and hemisegments of the salamander spinal cord at the cellular level, using a biophysical model adapted from the lamprey literature (Bicanski et al. 2011, 2012, in the same issue). The neuron model was a simplified version of the multicompartment Hodgkin-Huxley model used by Wallén et al. (1992) (reduced from 5 to 3 compartments). Current conservation yields the membrane potential of all compartments.

$$C\frac{\mathrm{d}U}{\mathrm{d}t} = \sum_i (U_i - U)g_{\text{core}} + \sum_j I_j + I_{\text{leak}} + I_{\text{SYN}}, \quad (1)$$

where the first sum is taken over adjacent compartments. The sum over j indicates summation over compartmental currents. The currents were modeled with standard Hodgkin-Huxley equations of the type

$$I_j = g_j p^{\text{a}} q^{\text{b}} (U_i - E_{\text{rev}}) z \quad (2)$$

Here g_j is the conductance of the ionic channel, p^a and q^b its activation and inactivation variables with their respective exponents and E_{rev} the reversal potential of the charge carriers in question. For currents which depend on the intracellular calcium concentration p and q are set to 1 and z (otherwise equal to 1) is a concentration-dependent activation variable. Intracellular calcium concentrations were modeled with an equation of the type

$$\frac{d[Ca]}{dt} = AI - B[Ca] \tag{3}$$

with inflow and decay parameters A and B. The intracellular calcium concentration was transformed into the activation variable via the following equation.

$$z = \frac{[Ca]}{B_z} \tag{4}$$

B_z is a scaling parameter. Synaptic conductances were raised instantaneously to their maximum value upon detection of a presynaptic spike and then decayed exponentially. An NMDA bath could be simulated by activating a tonic transmembrane conductance, subject to a voltage-dependent magnesium block, which mimicked a steady-state fraction of docked agonist.

The circuit architecture used was strongly inspired by that previously deciphered for the lamprey segmental swimming CPG axial circuit. Our circuit included on each side a pool of recurrently connected excitatory neurons projecting ipsilaterally to a pool of inhibitory neurons that in turn inhibit all neurons contralaterally. Excitatory neurons also project contralaterally to excitatory neurons (cf. Fig. 1C). Despite the absence of anatomical data for these neurons in the adult salamander, evidence has been provided that neurons in the spinal cord of the larval *Triturus vulgaris* (the smooth newt) show some typical anatomical characteristics of locomotor excitatory and inhibitory neurons populations described in other axial networks, including the lamprey (Harper and Roberts 1993, for review see Ryczko et al. 2010b).

Our network model reproduces rhythmic bursting that is generated by isolated segments and hemisegments when activated with NMDA, as well as most of the pharmacologically-induced modifications of the motor pattern observed experimentally in the salamander (Ryczko et al. 2010a). Interestingly, driving the modeled spinal segments with excitatory inputs from simulated reticulospinal neurons yields fast oscillations covering the frequency range observed during swimming in salamanders. Furthermore, a minimal modification of conductance parameters (e.g., controlling Ca^{2+} inflow and decay rates) in the spinal neurons, yields a slower frequency range similar to that observed during in vivo stepping. Blocking reciprocal inhibition in our model abolished rhythms under these in vivo-like conditions. Thus, the model predicts that in the salamander, left-right reciprocal

coupling is not needed to generate rhythmic activity in hemisegments activated with NMDA, but may be required to generate in vivo locomotor activity. This corroborates the observation in the lamprey that a surgical separation of the left and right hemicords abolished the locomotor activity elicited by electrical stimulation of the brain (Jackson et al. 2005). Interestingly, the main burst-terminating conductance under in vivo-like conditions (K_{CaN}) was originally included in the model following our in vitro demonstration of its involvement in the rhythmic activity generated under NMDA drive in isolated spinal segment of the salamander locomotor network (Ryczko et al. 2010a). Hence, though caution is warranted when interpreting in vitro data, such data can be informative of the operation of the network in vivo. In addition the simulations allowed us to propose a coupling mechanism at the cellular level, which can explain the synchronization of limb and axial networks, as is likely the case during gait transitions from swimming to stepping. Taken together, these results give further support to the hypothesis that the basic design of the axial CPG has been conserved during evolution, albeit with species-specific differences.

2.2 The tail networks

The information concerning the networks controlling the tail movements in the salamander is scarce. So far, most of the neurobiological studies that examined the functioning of axial movements in salamanders have targeted the trunk segments. However, in recent kinematic and EMG studies we provided evidence that the salamander's tail plays an active role during locomotion on land (acting as a "fifth limb") (Ryczko 2008; Charrier et al. 2010; Charrier and Cabelguen 2011). Tail movements facilitate dynamic balance during stepping on a slippery surface. Interestingly, the tail musculature displays a complex and variable EMG pattern during straight land stepping. Depending on the nature of the surface on which the animal evolves, one or two bursts per cycle can be observed in tail muscles (Fig. 2). The second burst is of lower amplitude and occurs simultaneously with the main burst generated contralaterally, thus providing a typical example of co-contraction of the left-right muscles. In contrast, independently of the nature of the surface, the trunk musculature displays a much more stable EMG pattern, with a single burst by cycle alternated between left and right sides (Fig. 2).

Interestingly, recent electrophysiological experiments revealed that a spinal CPG for tail movements (i.e., a "tail CPG"), consisting of a double chain of oscillators, is present in the tail spinal segments (Charrier and Cabelguen 2011). This architecture is similar to that of the axial CPG examined in the trunk (Ryczko et al. 2010a). However, although this similarity can explain the left-right alternation and the
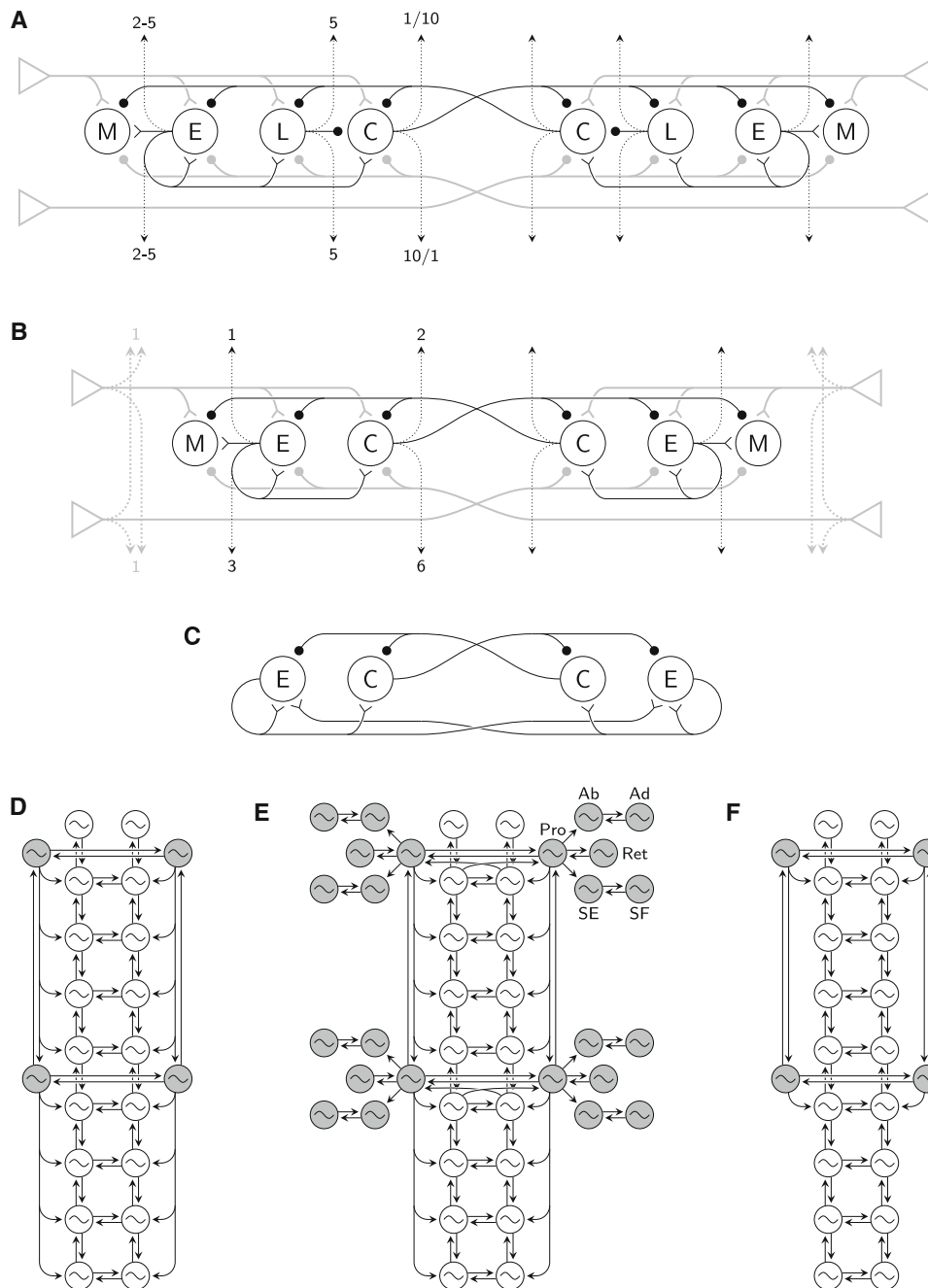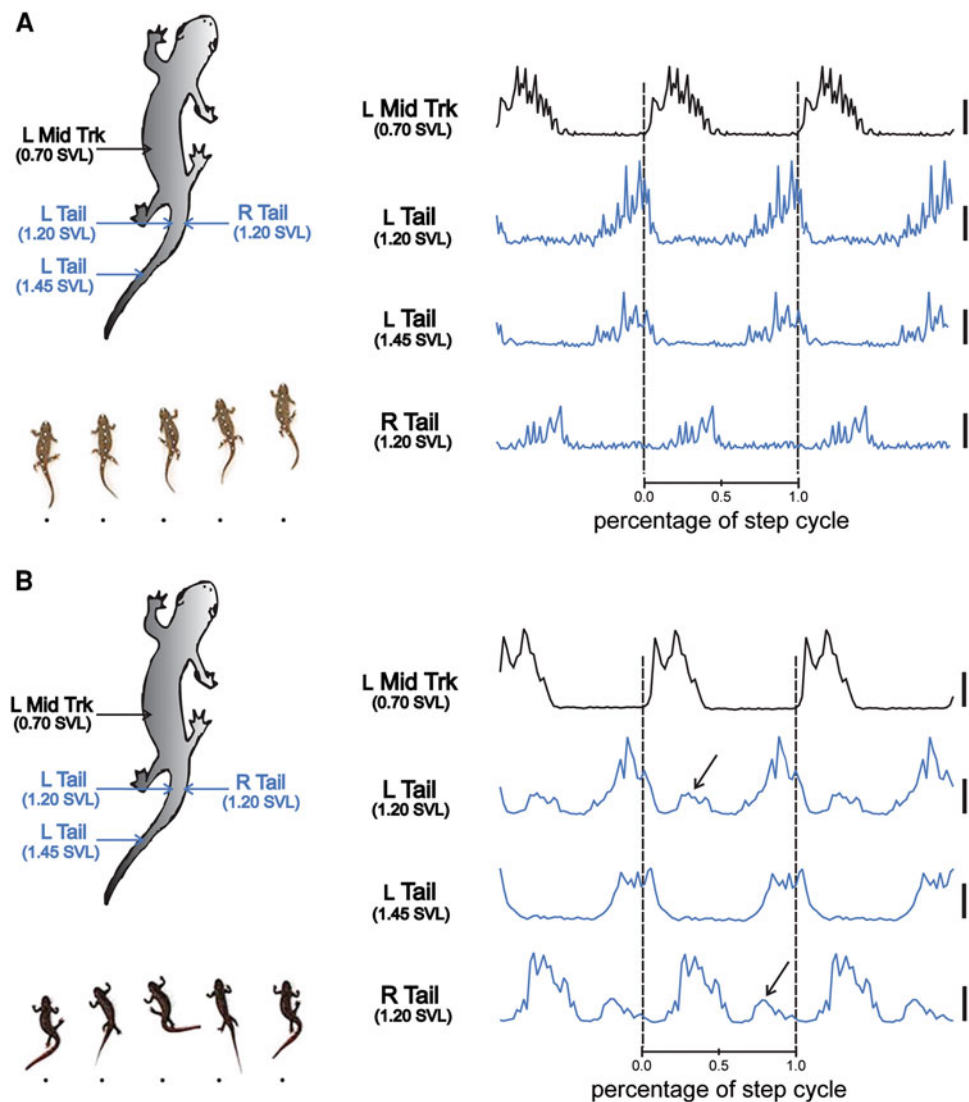
Fig. 1 Models of the salamander spinal circuitry for locomotion. **A** Segmental network in Bem et al. (2003). Four populations of non-spiking neurons are present in the left and right side of the spinal cord: motoneurons (*M*), excitatory interneurons (*E*), inhibitory interneurons projecting ipsilaterally (*L*), and inhibitory interneurons projecting contralaterally (*C*). Stretch-sensitive edge cells (*gray triangles*) send excitatory connections to ipsilateral populations and inhibitory connections to contralateral populations. The *E* and *L* populations have axons extending ipsilaterally to 2–5 and 5 segments respectively, in both directions. The *C* population has axons extending to 1 segment rostrally and 10 segments caudally; these extents were reversed in the rostral part of the spinal cord to reproduce EMG recordings of the walking trot. **B** Segmental network in Harishandra et al. 2011, employing integrate and fire neurons. Both *E* and *C* populations have axons extending longer in the caudal direction. **C** Segmental network in Bicanski et al. (2012).

The *E* populations also project to the contralateral *E* population. Model neurons are of the Hodgkin-Huxley type. **D** A CPG network with global coupling between limb and axial oscillators, as used in Ijspeert et al. (2005) and Ijspeert et al. (2007). Axial and limb oscillators are represented in white and gray, respectively. The Ijspeert et al. (2005) model has 40 segments while Ijspeert et al. (2007) has 8. **E** A CPG network with global ipsilateral limb → body coupling and local contralateral body → limb coupling, as used in Harishandra et al. (2011). Each limb is modeled with separate oscillators for the following muscles: abductor (*Ab*), adductor (*Ad*), protractor (*Pro*), retractor (*Ret*), shoulder or knee extensor (*SE*), and flexor (*SF*). The model includes 40 segments but only 9 are shown. **F** A CPG network with local coupling between limb and axial oscillators, as used in Ijspeert et al. 2005 and Knuesel and Ijspeert 2011. These models include 40 segments but only 9 are shown.

Fig. 2 Representative EMG patterns and sequence of snapshots during straight stepping on a non-slippery surface (**A**) and on a slippery surface (**B**). For each channel, EMG activity was full-wave rectified, filtered, and averaged over $n = 5$–10 consecutive stepping cycles. The *arrows* in **B** indicate the additional burst per cycle displayed by the proximal part of the tail musculature. *Insets* on the *left* indicate electrode locations specified as fraction of the snout vent length (SVL). Sequences of snapshots show one complete stride (lasting 1,080 ms in **A**, and 1,680 ms in **B**). Sequences progress from *left* to *right* (Adapted from Charrier et al. 2010).

waves of EMG activity travelling along the tail muscles during land stepping (Delvolvé et al. 1997), it does not explain the double bursting pattern which can occur selectively in the tail during stepping in an unstable environment. How these variable tail patterns are generated remains to be determined. Some properties of the tail CPG may be different from that of the trunk. The weak cross-excitatory connections, observed in the trunk CPG (Ryczko et al. 2010a) could also be present in the tail CPG. These connections may selectively be activated in the tail during stepping on a slippery surface, and thus contribute to the double burst pattern observed in the tail. More experiments are needed to reveal whether descending and/or sensory inputs specific to the tail network do play a role. Taken together, these preliminary results suggest that the salamander can control trunk and tail differentially during stepping (Charrier and Cabelguen 2011).

2.3 The limb networks

The neural organisation of the limb networks is not fully deciphered in salamanders. It is worth to note that the idea of phylogenetical conservatism may be extended to the limb CPGs (Grillner 2011), since some typical characteristics of the limb electromyographic patterns during locomotion, which are well-characterized in various vertebrates, are present in newborn babies, and retained during development until adulthood (Dominici et al. 2011). In salamanders, the forelimb CPG is better understood than the hindlimb CPG (reviewed in Chevallier et al. 2008). According to electrophysiological and anatomical data, the forelimb CPG appears to be composed of a set of independent oscillators (i.e., unit burst generators) for flexor and extensor muscles, which are coupled with inhibition in parallel with weaker excitation (Cheng et al. 1998, 2002; Jovanovic et al. 1999; Lavrov and Cheng

2008). Anatomical data suggest that left and right limb networks may also interact, as interneurons with a commissural axon ventral to the central canal were observed in the forelimb segments (Jovanovic and Burke 2004). Rhythmogenesis in the forelimb networks involves glutamatergic neurotransmission mediated by NMDA receptors (Wheatley and Stein 1992; Wheatley et al. 1992, 1994; Lavrov and Cheng 2004).

The neural mechanisms underlying the coupling between the limb CPGs and the axial CPGs in the salamander are still unknown. However, three important experimental findings are worth mentioning since they constrain modeling studies of the mechanisms underlying gait transitions: (i) rhythmic movements of each forelimb can be generated by an independent hemisegmental oscillatory network (Brändle and Székely 1973; Székely and Czéh 1976; Cheng et al. 1998); (ii) the intrinsic frequency of the limb CPGs is lower than that of the axial CPG (Ijspeert et al. 2007); (iii) experiments on isolated spinal cords have shown that the axial CPG can produce traveling waves even when the limb CPGs are rhythmically active (Ryczko et al. 2009). This is consistent with a coupling of limb oscillators mainly to the nearest axial oscillators (i.e., local coupling, as opposed to global coupling to large parts of the axis) (Ijspeert et al. 2005). It is known that during swimming, when limbs are tonically active, the rostrocaudal traveling EMG wave shows irregularities in the phase lag near the girdles (Delvolvé et al. 1997; Bem et al. 2003). The simulation study by Bem et al. (2003) suggests that limb activity, or a difference in local sensory feedback compared to rest of the axis, leads to the lag discontinuities observed in vivo (see Sect. 3.2). However, the local influence of limb-to-trunk connections on the phase lag along the axis during phasic limb activity has so far not been explored systematically.

3 Spinal mechanisms underlying gait transitions

Salamanders display two principal locomotor modes, stepping and swimming. Most likely the ability to switch between locomotor modes or gaits involves intrinsic properties of the spinal networks, sensory feedback, and supraspinal influences. In the present section we will describe how intrinsic properties of the spinal CPG and sensory feedback may contribute to various gait transitions, and how these aspects were investigated with models. These elements are reviewed keeping in mind that the switch from stepping to swimming can be controlled simply by increasing the electrical stimulation of a supraspinal structure, the mesencephalic locomotor region (reviewed in Sect. 4).

3.1 A central mechanism for switching between swimming and stepping

We investigated spinal mechanisms underlying the gait transition from swimming to stepping by combining a mathematical model of the locomotor circuitry coupled with a mechanical model of the body, i.e., an amphibious salamander-like robot (*Salamandra robotica*) (Ijspeert et al. 2007). The CPG model was composed of amplitude controlled phase oscillators. The state variables of individual oscillators are given by the following equations.

$$\dot{\theta}_i = 2\pi v_i + \sum_j r_j w_{ij} \sin(\theta_j - \theta_i - \phi_{ij}) \tag{5}$$

$$\ddot{r}_i = a_i \left(\frac{a_i}{4}(R_i - r_i) - \dot{r}_i \right) \tag{6}$$

$$x_i = r_i(1 + \cos \theta_i) \tag{7}$$

Here θ_i and r_i represent the phase and amplitude of the oscillator i. v_i and R_i determine the intrinsic frequency and amplitude, and a_i is a positive constant. The weights between oscillators and the phase bias were set by w_{ij} and ϕ_{ij}. Note that here the phase-response curve of the coupling term appears explicitly in Eq. 5, as the sine of the phase difference offset by ϕ_{ij}. The positive oscillatory signal x_i represents the burst produced by the oscillator.

The structure of the CPG relied on four hypotheses. (i) The axial CPG of the salamander is organized like that of the lamprey, i.e., as a double chain of oscillators (here, with symmetric weights, antisymmetric phase biases, and diffusive nearest neighbour couplings, see Fig. 1 and Eq. 5) and is able to generate traveling waves similar to that observed during swimming. This prediction was confirmed experimentally—in part a posteriori—in the salamander (Delvolvé et al. 1999; Ryczko et al. 2009, 2010a). The biological basis for assuming nearest neighbor coupling between oscillators relies on the following observations. First, a single axial hemisegment of the salamander can generate rhythmic activity in vitro (Ryczko et al. 2010a) as previously observed in the lamprey (Cangiano and Grillner 2003). Second, a single axial segment of the salamander is able to generate left-right coordinated activity (Ryczko et al. 2010a). Since a segment is constituted by two hemisegments coupled with their respective nearest neighbor (i.e., the contralateral hemisegment), this suggests that the nearest neighbor coupling is sufficient at the segmental level to produce coordinated activity. A similar simple assumption can be made for rostrocaudal coordination, since small pieces of the spinal cord of the salamander (i.e., 2 segments) can produce a left-right coordinated activity, together with a near

synchronous activity on ipsilateral ventral roots (Delvolvé et al. 1999). Of course, this coupling scheme is an approximation and does not represent the complexity of the short and long range couplings that may be present in the spinal locomotor network of the salamander (Ijspeert et al. 2005). (ii) A strong unilateral and global coupling from limb oscillators to axial oscillators allows the limb oscillators to impose their frequency on the axial network when limbs are activated (cf. Fig. 1D). This coupling generated a standing wave during stepping as observed in vivo (Delvolvé et al. 1997). However, this hypothesis needs to be revised in the light of our recent neurobiological data suggesting that the coupling between limb oscillators and axial CPG is mainly local, and not global (Ryczko et al. 2009). (iii) The limb oscillators cannot oscillate at high frequencies, i.e., they saturate at high levels of stimulation. Although not observed so far in the salamander, interestingly this saturation phenomenon has been observed in the Xenopus limb networks for a high pharmacological drive (Rauscent 2008). (iv) For the same drive, limb oscillators have a lower intrinsic frequency than the axial oscillators. This hypothesis has been confirmed experimentally in the salamander (Ijspeert et al. 2007).

Our numerical simulations demonstrated that when varying the descending drive (that is homogeneously provided to all oscillators), this simple circuitry was successful in generating the main features of swimming and stepping, and the transition between these modes in accordance with the results obtained when stimulating the MLR experimentally (Cabelguen et al. 2003). The saturation of the limb oscillators for a high drive provides a mechanism for automatically switching between stepping (at low MLR drive) and swimming (at high MLR drive). This saturation of the limbs also explains why swimming frequencies are systematically higher than stepping frequencies in kinematic recordings of freely moving animals (Frolich and Biewener 1992; Delvolvé et al. 1997). The difference in the intrinsic frequencies of limb and axial oscillators provides an explanation for the rapid increase of frequency during the switch from stepping to swimming. Indeed, for a low descending drive, the limb oscillators slow down the axial rhythm during stepping. Once silenced by a higher drive, the limb oscillators rapidly release the intrinsically faster axial oscillators from their influence, thus allowing thus the axial oscillators to generate the swimming rhythm at a higher frequency.

We then asked whether this model of the locomotor circuitry was able to generate swimming and stepping with controlled speed and direction in a real environment. As this examination required a mechanical body, the CPG model was implemented on an amphibious salamander robot that was composed of axial segments and rotational limbs (*Salamandra robotica*). Turning was achieved by applying a left-right asymmetrical drive on the CPG. The robot turned in
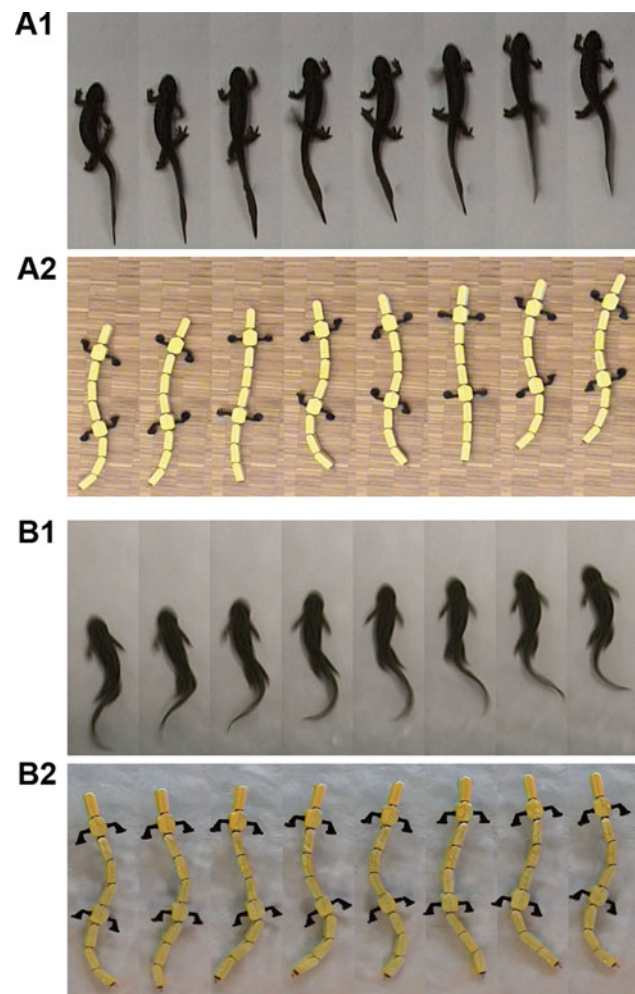

Fig. 3 Comparison of animal and robot locomotor modes. **A** Stepping kinematics of the salamander (**A1**) and the robot (**A2**). **B** Swimming kinematics of the salamander (**B1**) and the robot (**B2**) (Adapted from Ijspeert et al. 2007).

the direction of the side receiving the highest drive. This was due to an increase of the amplitude of the oscillations on the side receiving the higher drive, thus generating a transient offset in the set points sent to the joint motor controllers. The robot constituted a unique opportunity to study the interactions between a simulated nervous system and the mechanics of a body in various environments, something that cannot be achieved when studying the different components in isolation. The robot allowed us to qualitatively and quantitatively demonstrate that the swimming and stepping gaits generated by the robot, controlled by the CPG model, were close to the gaits of the real salamander (for instance by comparing kinematic data such as lateral displacements of the animal and the robot, cf. Fig. 3). As such, our model of the salamander locomotor circuitry could account for two locomotor programs observed in the real animal.

3.2 The role of sensory feedback in the gait transition from swimming to stepping

In Ijspeert et al. (2007) the generation and change of gait was hypothesized to be a purely central mechanism, i.e., it was produced without any sensory feedback such as the proprioceptive signals due to the actual movements of the body and limbs. However, rhythmic and tonic sensory inputs have a major influence on the CPG for locomotion (for review, see Rossignol et al. 1998, 2006) to adjust the locomotor movements to the internal goals and external conditions.

In the lamprey, intraspinal mechanosensitive neurons ("edge cells") have been shown to provide movement-related feedback input to the swimming CPG (Grillner et al. 1982, 1984). During swimming in lampreys, ipsilateral stretching of the cord activates the ipsilateral edge cells. In turn, the edge cells send excitatory inputs ipsilaterally to facilitate the activation of the stretched hemisegment, and send inhibitory inputs to the contralateral side, thus contributing to the termination of the activity of the contralateral hemisegment (Wallén and Grillner 1997).

In salamanders, intraspinal marginal neurons distributed all along the ventro-lateral edge of the spinal cord (Schroeder and Egar 1990) show strong similarities with the edge cells of lampreys. Although the stretch responsiveness of these cells remains to be determined, exploratory modeling studies have been performed to examine how this putative intraspinal stretch receptor system may influence the locomotor CPG of the salamander.

In a first study, some of us examined whether local input drives fed into an axial network inherited from the lamprey could contribute to generate the typical motor patterns underlying swimming and stepping in the salamander (Bem et al. 2003). The neuromechanical model consisted of a lamprey swimming circuitry built with non-spiking neurons, no limb networks, and a mechanical model of the lamprey body (after Ekeberg 1993) (Fig. 1A). Model neurons represented entire populations and their mean firing frequency was given by

$$u = 1 - \exp\left[(\theta - \xi_+)\Gamma\right] - \xi_- - \mu\vartheta \tag{8}$$

if positive and 0 otherwise. Here Γ is a gain constant, ϑ implements delayed negative feedback, representing spike-frequency adaptation, scaled by μ, and $\xi_{+/-}$ are the delayed summed excitatory and inhibitory synaptic inputs, respectively.

$$\dot{\xi}_+ = \frac{1}{\tau_D}\left(\sum_{i \in \Psi_+} u_i w_i - \xi_+\right) \tag{9}$$

$$\dot{\xi}_- = \frac{1}{\tau_D}\left(\sum_{i \in \Psi_-} u_i w_i - \xi_-\right) \tag{10}$$

$$\dot{\vartheta} = \frac{1}{\tau_A}(u - \vartheta) \tag{11}$$

Visco-elastic muscles drove 10 mechanical body segments, connected by 9 joints. The torque T_i acting on a given joint i was assumed to be a linear function of the motoneuron activity on the two sides of the body, M_L and M_R.

$$T_i = \alpha(M_L - M_R) + \beta(M_L + M_R + \gamma)\varphi_i + \delta\dot{\varphi}_i \tag{12}$$

Here α is the gain of the muscles, β the stiffness gain, γ the tonic stiffness, and δ is a damping coefficient. φ_i refers to the joint angle. The activity of stretch receptors was proportional to the local body curvature on the stretched side, and zero on the other side.

This simulation study suggests that to generate the salamander stepping EMG pattern with standing waves in the trunk occurring together with a double bursting in the girdle regions (Delvolvé et al. 1997), the network must receive a tonic excitatory drive at the girdles and a phasic excitatory drive which is out of phase in the neck and tail regions in relation to the trunk. This phasic drive mirrored the local curvature of the body since its intensity was calculated as an output from the stretch sensitive receptors (i.e., edge cells). The salamander swimming pattern, with two discontinuities observed near the girdles in the EMG traveling waves (Delvolvé et al. 1997), appeared when the axial network received a tonic excitatory drive together with local variations (i.e., increase or removal) in the excitatory drive produced by the stretch receptors near the girdle regions. This simulation study suggested that the local input drives involved in the generation of particular features of the stepping and swimming patterns could be attributed to local variations of activity of the edge cells and/or the limb networks.

In a second study, some of us used a neuro-mechanical model of the salamander to examine the involvement of sensory feedback in the switch from traveling to standing wave observed during the transition from swimming to stepping (Ijspeert et al. 2005). The CPG models were based on coupled nonlinear oscillators rather than neural networks to reduce the number of model parameters and state variables (cf. Fig. 1D–F). The axial network consisted of a double chain of identical oscillators coupled to the nearest neighbors. Dominantly rostrocaudal, balanced and dominantly caudorostral intersegmental connections were explored. All three types of coupling could generate traveling waves, but in the balanced case the resulting patterns converged more slowly towards the traveling wave. Individual oscillators were governed by the following equations,

$$\tau\dot{v}_i = -\alpha + \frac{x_i^2 + v_i^2 - E_i}{E_i}v_i - x_i$$
$$+ \sum_j (a_{ij}x_j + b_{ij}v_j) + \sum_j c_{ij}s_j \tag{13}$$

$$\tau \dot{x}_i = v_i \tag{14}$$

with $\tau, \alpha, E, a_{ij}, b_{ij}$ constants. The latter two determine how oscillator j influences oscillator i. s quantifies the sensory input weighted by c_{ij}. Variations in the couplings between the limb and the axial network (i.e., global vs. local; unidirectional vs. bidirectional) and between fore- and hindlimb networks (with/without) were explored in this study. A mechanical body of the salamander was designed as an extension of the mechanical simulation of the lamprey body (after Ekeberg 1993). A minimal model of sensory feedback was designed by distributing stretch receptors on both sides of each joint of the mechanical body. These simulated edge cells produced a signal proportional to the local stretch that was fed onto the axial network. The effect of incorporating sensory feedback in the different CPG configurations was explored in the context of the gait generation. Without sensory feedback, the stepping standing waves were generated by the CPG only when a global coupling between the limb and axial oscillators was present. Indeed, when only a local coupling from the limbs to the closest axial oscillators was present, traveling waves were propagated in the axial network due to its intrinsic coupling structure. But interestingly, using the same drives and CPG configuration when the body was in contact with the ground (i.e., not in water) yielded a mechanical standing wave in the trunk and the tail, as has been observed in the lamprey moving on a wet bench (Bowtell and Williams 1991). In this situation sensory signals from the edge cells would reflect the standing wave, despite the traveling wave being sent to the muscles by the axial network. In fact the introduction of sensory feedback led to a decrease in the intersegmental phase, so that the activity pattern approached a standing wave. This illustrates that sensory feedback from the edge cells could indeed contribute to the generation of the standing wave observed in vivo in the axial EMG recordings. In other words, sensory feedback combined with different properties of physical interactions between the body and the environment could in principle explain the switching between traveling waves in water and standing waves on ground.

Interestingly, the sensory feedback increased the frequency of oscillations in the simulations of Ijspeert et al. (2005). Though this property was so far not explored systematically, it is in accordance with the observation that fictive locomotion usually generates frequency ranges that are lower than real locomotion in the salamander (Delvolvé et al. 1997; Delvolvé et al. 1999). This phenomenon may be related to an increased excitability of the spinal locomotor network, probably caused by the activity of sensory neurons during actual locomotion. Isolated lamprey spinal cords with muscles attached (i.e., allowing the preparation to move and thus to generate sensory feedback) generate a rhythmic activity of higher frequency than

that of isolated spinal cords (Guan et al. 2001). Furthermore rhythmic bending of the isolated lamprey spinal cord can induce a long-lasting increase of the frequency of the CPG's activity (Kiemel and Cohen 2001). In the lamprey these effects could involve e.g. the intraspinal mechanosensitive edge cells (Grillner et al. 1982, 1984). In the turtle, activation of the cutaneous afferents and sensory neurons induce a long lasting increase of spinal interneurons involved in the scratch reflex (Currie and Stein 1990). In the salamander, the neural mechanisms underlying this phenomenon remain to be explored.

We have recently investigated a novel hypothesis involving the role of the muscles dynamics and sensory feedback in the emergence of a standing wave of EMG activity during stepping. Our recent results have shown that traveling waves of activity in the trunk, and limb activity can occur simultaneously in the isolated salamander CPG (Ryczko et al. 2009), suggesting that the coupling from limb oscillators to axial networks is mainly local, as in some configurations of the CPG proposed in Ijspeert et al. (2005). Knuesel and Ijspeert (2011) used a neuro-musculo-mechanical model of salamander to investigate the possible role of muscle dynamics and sensory feedback in the shaping of the kinematic and CPG pattern. The model uses abstract Hopf oscillators for the CPG, with local couplings from limb to body oscillators (cf. Fig. 1F). Muscles and stretch receptors are modeled similarly to (Bem et al. 2003). The Hopf oscillators were connected with diffusive couplings (similarly to Ijspeert et al. 2007), and governed by the following equations,

$$\dot{\theta}_i = 2\pi v_i + \sum_j r_j w_{ij} \sin(\theta_j - \theta_i - \varphi_{ij}) \tag{15}$$

$$\dot{r}_i = \gamma (R_i^2 - r_i^2) r_i \tag{16}$$

and rewritten in Cartesian coordinates (van den Kieboom 2009) to incorporate feedback:

$$\dot{x}_i = \gamma (R_i^2 - r_i^2) x_i - \bar{\omega}_i y_i + w^{\text{ipsi}} s_i^{\text{ipsi}} + w^{\text{contra}} s_i^{\text{contra}} \tag{17}$$

$$\dot{y}_i = \gamma (R_i^2 - r_i^2) y_i + \bar{\omega}_i x_i \tag{18}$$

$$\bar{\omega}_i = \omega_i + \sum_{j=1}^N \frac{w_{ij}}{r_i} \left[(x_i y_j - x_j y_i) \cos \varphi_{ij} - (x_i x_j + y_i y_j) \sin \varphi_{ij} \right] \tag{19}$$

Here ω_i is the angular frequency, R_i the target amplitude, γ is a convergence factor, w_{ij} specifies the coupling weights and ϕ_{ij} the phase bias. For the left side, the sensory inputs s^{ipsi} and s^{contra} denote the positive parts of φ_i and $-\varphi_i$ respectively, with φ_i being the angle of the joint acted upon by the muscle model (φ_i and $-\varphi_i$ are exchanged for the right side). The

torque acting on each joint is calculated from Eq. 12, using the positive part of y_i for the motoneuron activity.

This CPG model employed symmetrical weights and anti-symmetrical phase biases, to produce rostrocaudal traveling waves of muscle activity in the absence of sensory feedback. Stepping was simulated in this condition, using a broad range of muscle elastic and damping properties. Two regions of the muscle parameter space were found to give good locomotion performance: one, with lower body stiffness, where the kinematics closely followed the muscle activation pattern, and another, with higher body stiffness, where the trunk kinematics approaches a standing wave in spite of a traveling wave of muscle activation. Using muscle parameters from the second region, the effect of local sensory feedback on the CPG was explored with a broad range of ipsilateral and contralateral feedback strengths. A region was found where sensory feedback has a strong modulatory effect on the CPG, leading to an activity pattern resembling a standing wave in the trunk. An interesting aspect of this preliminary work is that it suggests how the animal can shape the mechanical wave during land locomotion by adjusting its body stiffness. This is in line with the observation that trunk muscle contractions are stronger during terrestrial trotting than during aquatic trotting in the salamander *Ambystoma maculatum*, thus suggesting increased body stiffness during terrestrial trotting (Deban and Schilling 2009). This increase in body stiffness may modify the mechanical wave along the trunk, as suggested by the differences in the bending profile of the trunk that have been observed when comparing aquatic and terrestrial walking on an inclined ramp in the newt *Taricha torosa* (Ashley-Ross and Bechtel 2004). Altogether these data support the idea that body stiffness plays an important role in adapting the body mechanics during locomotion, as suggested in an elegant computational study of the interactions between fluid dynamics and a neuromechanical model for lamprey swimming (Tytell et al. 2010).

3.3 Switching from overground walking to trotting

Like most quadrupeds, salamanders display different locomotor gaits overground (see Table 1). At slow speeds, a walking gait is often adopted, presumably because it provides stable support throughout the step cycle. In this gait, one foot is lifted off the ground at a time, allowing for the remaining three to support the body. At higher speeds, salamanders can switch to a trotting gait where diagonally opposite feet are lifted simultaneously. This allows for faster locomotion but sacrifices the stability offered by the walking gait (Ashley-Ross et al. 2009).

Producing a coordinated gait is not just a matter of lifting the feet in the appropriate sequence. The footfall must also be properly synchronized with the axial movements to be efficient. The salamander uses axial undulations to increase

the stride length by timing the lift-off and touchdown of each foot with the times when the girdle is at an extreme angle. Switching from walking to trotting therefore has implications also for the activation patterns of the axial muscles of the trunk.

The mechanisms underlying the switching between different overground locomotor modes in the salamander have so far been investigated only in simulation. We have developed a three-dimensional mechanical model of the salamander body (*P. waltlii*) which allowed for the simulation of different coordination patterns (Harishandra et al. 2010). The model has more degrees of freedom than earlier models, and in particular, the legs included two degrees of freedom, one in the hip/shoulder joint and one in the knee/elbow joint. The simulated body was actuated by visco-elastic model muscles that were driven by motoneuron activation patterns, which were generated with time driven functions rather than using a simulated spinal network. The output of these heuristic pattern generators was calculated from the following equations.

$$E_p(t, i) = A \left\| \sin^3(2\pi f t + \phi_1) \right\| \tag{20}$$

$$E_r(t, i) = A \left[1 - \left\| \sin^3(2\pi f t + \phi_1) \right\| \right] \tag{21}$$

for the limbs, where $E_p(t, i)$ and $E_r(t, i)$ are the inputs to the protractor (extensor) and retractor (flexor) muscles for joint i at time t. The maximum amplitude of the signal is given by A which may vary from joint to joint. f and ϕ_1 correspond to the frequency of oscillation and the phase at joint i, respectively. Similarly the muscles controlling the body (trunk and tail) receive an activity pattern that is of the form $E_p(t, i)$. The muscle model is based on the mathematical model introduced by Ekeberg (1993) in his neuro-mechanical lamprey model (see above). The calculation of the muscle torque is based on the following equation.

$$T = (\alpha + \beta \Delta\varphi)E + \gamma \Delta\varphi + \delta \Delta\dot{\varphi} \tag{22}$$

The torque acting at a particular joint is determined by the neural activation ('E') of the muscle, where $\Delta\varphi$ is the difference between the actual angle of the joint and the resting angle. The coefficients α, β, γ, and δ determine the characteristics of the muscle and muscle-joint combination and denote gain, stiffness gain, intrinsic stiffness, and a damping coefficient respectively.

By testing different temporal patterns of motoneuron activity, we could confirm that a standing wave in the trunk was appropriate for the trotting gait, as previously observed in vivo (Delvolvé et al. 1997) and in the salamander robot (Ijspeert et al. 2007). For the walking gait, however, a slight rostrocaudally traveling wave of muscle activation between the girdles proved optimal to match the footfall pattern. Whether a traveling wave of EMG activity occurs in the trunk of *P. waltlii* during walking remains

Table 1 The reported locomotor modes of salamanders

Locomotor mode	Species	Environment	Kinematics	Electromyograms
Forward swimming	Ambystoma maculatum	Tray filled with water	(T) Deban and Schilling (2009)	(T) Deban and Schilling (2009)
	Ambystoma mexicanum	Flow tank	(T) D'Août et al. (1996)	(T) D'Août et al. (1996)
	Ambystoma tigrinum	Flow tank	(T) Frolich and Biewener (1992)	(T) Frolich and Biewener (1992)
	Ambystoma tigrinum	Immersed trackway	(T) Bennett et al. (2001)	(T) Bennett et al. (2001)
	Dicamptodon ensatus	Trough	(T) Carrier (1993)	(T) Carrier (1993)
	Pleurodeles waltlii	Tank	(T) Ijspeert et al. (2007)	(T, L) Delvolvé et al. (1997)
	Siren intermedia[a]	Flow tank	(T) Gillis (1997)	*
	Siren lacertina[a]	Water-filled flat trackway	(T) Azizi and Horton (2004)	*
Terrestrial undulatory locomotion	48 species of terrestrial salamanders	Roughened flat surface	(T, L) Edwards (1977)	*
Forward terrestrial walking	Ambystoma tigrinum	Wet flat trackway	(T, L) Bennett et al. (2001)[b]	(T) Bennett et al. (2001)[b]
	Ambystoma tigrinum	Flat plate	(L) Peters and Goslow (1983)	*
	Dicamptodon ensatus	Wet trough	(T, L) Carrier (1993)	(T) Carrier (1993)
	Dicamptodon tenebrosus	Flat treadmill	(T, L) Ashley-Ross (1994a,b), (L) Ashley-Ross (1995); (L) Ashley-Ross and Lauder (1997)	(L) Ashley-Ross (1995); (L) Ashley-Ross and Lauder (1997)
	Taricha torosa	Dry 15° inclined ramp	(T, L) Ashley-Ross and Bechtel (2004)	*
	Taricha torosa	Flat treadmill	(T, L) Ashley-Ross et al. (2009)	*
	Triturus vulgaris	Presumably wet flat surface	(T, L) Roos (1964)[c];(T, L) Daan and Belterman (1968)[c]	*
	48 species of terrestrial salamanders	Roughened flat surface	(T, L) Edwards (1977)	*
Backward terrestrial walking	Dicamptodon tenebrosus	Flat treadmill	(T, L) Ashley-Ross and Lauder (1997)	(L) Ashley-Ross and Lauder (1997)
Forward terrestrial trotting	Ambystoma maculatum	Wet flat tray	(T, L) Deban and Schilling (2009)	(T) Deban and Schilling (2009)
	Ambystoma tigrinum	Flat treadmill	(T) Frolich and Biewener (1992)	(T) Frolich and Biewener (1992)
	Dicamptodon tenebrosus	Flat treadmill	(T, L) Ashley-Ross (1994a), Ashley-Ross (1994b)	*
	Pleurodeles waltlii	Wet flat surface	(T, L) Ijspeert et al. (2007)	(T, L) Delvolvé et al. (1997)
	48 species of terrestrial salamanders	Roughened flat surface	(T, L) Edwards (1977)	*
Forward aquatic walking	Siren lacertina[a]	Water-filled flat trackway	(T, L) Azizi and Horton (2004)	*
	Taricha torosa	Immersed 15° inclined ramp	(T, L) Ashley-Ross and Bechtel (2004)	*
Forward aquatic trotting	Ambystoma maculatum	Flat tray with water at mid-trunk height	(T, L) Deban and Schilling (2009)	(T) Deban and Schilling (2009)
	Taricha torosa	Immersed flat trackway	(T, L) Ashley-Ross et al. (2009)	*

T trunk data, L limb data

* No data

[a] Salamander with reduced forelimbs and no hindlimb

[b] Walk and trot have not been differentiated in this study

[c] The stepping pattern is described as crawling in this study, because the belly and the tail touch the ground

to be determined, as EMG patterns in this species have been recorded mostly during trotting (Delvolvé et al. 1997). Interestingly Karakasiliotis et al. (2012, same issue) have performed detailed three dimensional X-ray recordings of *P. waltlii* during walking and revealed that standing and rostrocaudal traveling waves can be differentially observed at various rostrocaudal levels in the trunk and tail. Patterns of motoneuron activity combining traveling and standing waves could underlie these complex kinematic patterns. Simulation suggests that the muscle properties could also contribute to transform a travelling wave of muscle activation into a mechanical standing wave (Knuesel and Ijspeert 2011).

Expanding upon the work presented in Harishandra et al. (2010), simulations were undertaken to investigate the organization of the neural network which coordinates the limbs and the axial undulations of the body during walking and trotting. We replaced the heuristic pattern generation (Eqs. 20, 21) by a spinal network consisting of a lamprey-inspired axial CPG (with dominantly caudal intersegmental connections, adapted from Kozlov et al. 2009) composed of populations of leaky integrate and fire neurons (Harishandra et al. 2011). The model neurons exhibit a fixed threshold, exponentially decaying postsynaptic conductances, conductance-based spike-frequency adaptation, a conductance-based relative refractory mechanism and a stochastic spread in passive properties (Muller et al. 2007). The neuron model can be described using a five-dimensional system of coupled differential equations as follows.

$$c_m \frac{dv(t)}{dt} = \beta_v(v(t), \ldots, g_r(t)) - (v_{th} - v_{reset})A(t) \quad (23)$$

$$\frac{dg_x(t)}{dt} = \beta_x(g_x(t), t) + q_x S_x(t) \quad (24)$$

$$\frac{dg_y(t)}{dt} = \beta_y(g_y(t), t) + q_y A(t) \quad (25)$$

where c_m represents the membrane capacitance, $g_x : x \epsilon \{e, i\}$, excitatory and inhibitory synaptic conductances, q_x *the* quantal conductance increase, $g_y : y \epsilon \{s, r\}$, the spike frequency adaptation and the relative refractory period, and q_y is the quantal conductance increase of the above mechanisms. $S_x(t)$ represents the excitatory and inhibitory input spike trains. If $v(t)$ exceeds the threshold, v_{th}, $v(t)$ is reset to v_{reset}. Analogous to the input spike train, $A(t)$ represents the output spike train. Note that, here

$$\beta_v(v, g_e, g_i, g_s, g_r) := g_l(E_l - v) + \sum_{\mu = e, i, s, r} g_\mu(E_\mu - v) \quad (26)$$

and for $\mu = e, i, s, r$,

$$\beta_\mu(g_\mu) := -\frac{1}{\tau_\mu} g_\mu \quad (27)$$

where g_l is the leak conductance, E_μ the various reversal potentials and τ_μ are the time constants. Body stretch receptor activation was modeled as current injection into the receptor neuron and was proportional to the local curvature of the body. The network model was augmented by a complex limb CPG, which provided the activation of multiple limb muscles. Limb stretch receptors were functioning as hip or scapula angle detectors. These receptor neurons increased their firing rate when a limb was extended more toward the caudal direction, i.e., at the later part of the stance phase. The following equation was used to calculate the required current to be injected into the receptor neuron.

$$i = \frac{k}{1 + e^{-2\Delta\theta}} \quad (28)$$

k is a proportionality constant and $\Delta\theta$ is the hip or scapula angle measured in the horizontal plane from an axis perpendicular to the axis along the body. It is positive and increasing in the direction of the retraction (late stance) and is negative and decreasing while protracting. The muscle model was the same as in Harishandra et al. (2010). The complete spinal network drove the body musculature, which generated the torques for the joints of our musculo-mechanical model of the salamander. Connections among the oscillators were not restricted to nearest neighbors. The limb CPGs were interconnected ipsilaterally and contralaterally and forelimb CPGs were coupled bidirectionally to the local neighbors of the axial CPG. Hindlimb-CPGs were connected to the body-CPG along the tail.

This model allowed us to examine in simulation the contribution of interlimb couplings and limb/axial couplings in the generation of trotting and walking gaits. We also tested the contribution that sensory feedback via stretch receptors, which detected the axial curvature and limb movements. The trotting gait could be generated centrally (i.e., without sensory feedback) by coupling the CPGs in accordance with earlier findings (Ijspeert et al. 2007), i.e., with a strong global coupling from limb to axial networks (Fig. 1D). The walking gait, however, could not be simulated without accompanying a reduced MLR drive by: (i) inclusion of sensory feedback, (ii) weakening the ipsilateral inter-limb couplings, (iii) using a strong, local, axial-to-limb coupling instead of the strong, global limb-to-axial coupling used during trotting.

These results suggested that the walking gait is relying on sensory feedback to a larger extent than trotting. This hypothesis must be tested in future experiments, but is consistent with the general trend that slow movements are often controlled via sensory feedback while fast movements are more often driven in a feed-forward mode (for review, see Pearson 1993). Importantly many neurobiological details regarding the spinal CPG are unknown (e.g. identity of neurons in the

network, connectivity of neurons, biophysical properties of neurons, nature of coupling, etc.), and therefore more data are needed to draw new conclusions regarding its organization/operation.

4 Supraspinal structures involved in locomotor control in salamanders

4.1 The mesencephalic locomotor region controls the locomotor frequency and the gait transition from swimming to stepping

Salamanders, as other vertebrates (Dubuc 2009), have a specific mesencephalic locomotor region (MLR) that controls the initiation and the maintenance of locomotion. The level of activation of that region determines the frequency and the mode of locomotion (Cabelguen et al. 2003). Stepping occurs during electrical microstimulation of the MLR at low intensity, whereas swimming requires higher intensities. This is consistent with swimming being the fastest mode of locomotion in these animals, which are mechanically better adapted for swimming than stepping due to their sprawling posture and short limbs (Ashley-Ross 1994a,b). This switch between stepping and swimming is reminiscent of the switch between walking, running, and galloping elicited in decerebrate cats when increasing the stimulation of the MLR (Shik et al. 1966). Similarly, transitions between walk, trot and gallop have been observed in decerebrate rats when increasing the stimulation of the MLR (Skinner and Garcia-Rill 1984). A similar transition from walk to gallop has been observed in the monkey when increasing the electrical stimulation of the vicinity of the cuneiform nucleus, considered to be part of the MLR (Eidelberg et al. 1981). Altogether these data suggest a conservatism of the MLR as a center controlling gait transitions in vertebrates. It is also worth noting that gait transitions from stepping to flight have been elicited in decerebrate birds by increasing the intensity of electrical stimulation of the pontomedullary reticular formation (Steeves et al. 1987).

There is anatomical and electrophysiological evidence in vertebrates that the MLR activates the spinal pattern generators for locomotion through the activation of reticulospinal neurons (see Dubuc et al. 2008; Le Ray et al. 2011 for review). It is likely that the descending influences from the MLR on the spinal locomotor networks in the salamander also involve brainstem reticulospinal neurons. Stimulation of the MLR in the roughskin newt *Taricha granulosa* elicited extracellularly recorded activity in the hindbrain that preceded the initiation of the locomotor bouts (Bar-Gad and Kagan 1999). Chronically implanted microwires in the reticulospinal region in the roughskin newt revealed an increased activity both during swimming or stepping (e.g. Hubbard et al. 2010, Lowry et al. 1996). Reticulospinal neurons have also been identi-

fied anatomically by injecting retrograde axonal tracers in the spinal cord (Hubbard et al. 2010). Some of these neurons are glutamatergic (Chevallier et al. 2004). Taken together these data are consistent with the idea that these neurons control the activity of spinal locomotor networks. Our recent modeling study suggests that the same spinal network could produce different frequencies depending on the descending pathway configuration that innervates it (Bicanski et al. 2012). However, so far it is unknown whether different reticulospinal cells and/or different cellular mechanisms are involved during MLR-induced stepping or swimming.

4.2 Turning

When salamanders are swimming, lateral turns are primarily produced by bending the body. This is an efficient way of steering during ongoing locomotion and is shared by most swimming vertebrates. Neural control of this kind of steering is relatively straightforward since a simple left-right asymmetry in activation of axial muscles along the body is sufficient to cause efficient turns during ongoing swimming (Ijspeert et al. 2007). In lampreys, some reticulospinal neurons located on the side of the turn increase their activity during turning (e.g. Deliagina et al. 2000; Fagerstedt et al. 2001), thus providing an asymmetry in descending inputs to the spinal network.

When the legs are used for locomotion, the limbs can play an active role in steering. In particular, salamanders actively use their forelimbs to side-step, i.e., to pull with the inner front limb and push with their outer front limb in a curve. By comparing the path followed when steering with side-stepping and pure body bending, using our musculo-mechanical salamander model (Harishandra et al. 2010), it is clear that side-stepping greatly improves manoeuvrability.

It is still an open question how the nervous system generates appropriate side-steps. Muscles controlling the elbow joints need to be partially activated in or out of phase with protraction and retraction. Since the necessary phasic activity is present at the spinal level in the limb CPGs, it is possible that a tonic steering signal from the reticular formation could act as a switch, which would be sufficient to control this kind of steering. Alternatively, the phasic signal may also originate from other supraspinal regions; opening up the possibility for more precise foot positioning using the same mechanisms.

4.3 Generation of complex movements

Documenting the diversity of behaviors in the salamander is an ongoing effort. Interestingly, locomotor movements restricted to the forelimbs, or to the hindlimbs, sometimes occur during episodes of underwater stepping in freely moving salamanders (Lamarque and Cabelguen, unpublished observations). Our current models fail to exhibit the
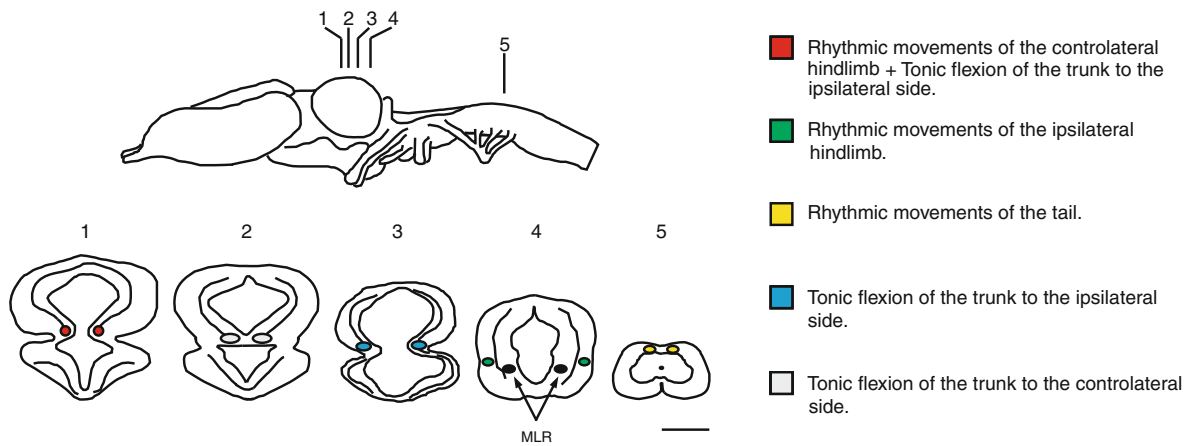
Fig. 4 Stimulation sites that evoked rhythmic and/or tonic movements of different parts of the body in the salamander *P. waltlii* (stimulation parameters: 2 ms pulses, 2.2–4.8 μA, 10–15 Hz). For comparison the MLR is also indicated. Schematic drawings of transverse sections show the distribution of the sites. The levels of the sections are indicated in the upper scheme. Calibration bar: 500 μm (Didier and Cabelguen, unpublished observations)

richness of salamander motor skills. In particular, questions remain whether subparts of our CPG model (i.e., a small set of oscillatory centers) can be activated independently of each other, in order to produce e.g. rhythmic movement of the forelimbs during swimming while the hindlimbs are folded against the body as was observed in some cases (Ryczko 2008). From a theoretical point of view, selective activation of a part of the spinal network can be obtained in different ways, including multiple descending pathways, finely tuned time-varying descending signals, additional spinal circuits, or time-varying connection topologies (for instance, under the influence of neuromodulators or by activating or inactivating relay centers).

We recently explored whether different descending inputs could selectively activate different muscular synergies in the semi-intact preparation of salamander (i.e., a decerebrated animal from which forelimbs were removed; Cabelguen et al. 2003). The investigation was motivated by the previous observation that in many species rhythmic movements of the axis or of the limbs/wings can be elicited by stimulation of sites distributed in the brainstem, the forebrain and the spinal cord (for review, see McClellan 1986; Grillner et al. 1997; Rossignol et al. 2006; Lemon 2008). For instance in the chick, wing flapping or stepping could be elicited independently, depending on the stimulation location, in the lateral funiculus at the level of the cervical spinal cord (Jacobson and Hollyday 1982). Interestingly, it has been suggested that in fish the axial and the pectoral fin CPGs for swimming are subjected to independent descending controls from the brain (Uematsu and Todo 1997). We have recently observed in the salamander that electrical microstimulation of various brain sites that are distinct from the MLR can induce rhythmic movements restricted to a single hindlimb (cf. Fig. 4) (Didier and Cabelguen, unpublished observations). Stimula-

tion of other sites could induce tonic bending of the whole body towards the left or the right, as would be needed for turning. Rhythmic movements restricted to the tail could be induced by electrical stimulation of the dorsal part of the first spinal cord segment, close to the obex.

These preliminary results support the view that the CNS could simplify the control of many degrees of freedom of the musculo-skeletal system by activating a small number of specific descending pathways, which in turn activate subsets of motor modules within the spinal cord (reviewed in Bizzi et al. 2008). This modularity can be seen as a mirror image of the proposed modularity in the spinal cord itself. In this context Bizzi et al. (2000) illustrated interesting experimental findings. Recording the muscle output of a frog with a fixated limb after stimulation of specific spinal areas revealed a response that depended on the position of the limb. Such experiments yield a so-called force field in space (for different limb positions and for the same spinal stimulation target). These force fields can change with the site of stimulation in the spinal cord. Combined stimulation of different sites apparently yields a simple linear superposition of the individual force fields (Mussa-Ivaldi et al. 1994). Furthermore it has been be confirmed (Giszter et al. 1993; Saltiel et al. 1998) that the evoked movements were a consequence of spinal interneuron activity (elicited either electrically or by NMDA) and not due to random motorneuron activation, direct stimulation of sensory afferents or descending projections. Similar findings have been reported in rats (Tresch and Bizzi 1999).

The hypothesis built on these findings states that the spinal cord comprises a set of behavioral modules, which can be combined to produce complex movements. This paradigm can be extended to the brainstem control system (D'Avella and Bizzi 1998). The notion that complex movements are

composed from a catalog of simpler stereotypical components (muscle synergies) is also reminiscent of the unit burst generator concept (Grillner 1981). The obvious advantage of composing complex movements from a limited pool of synergies is the simplification of control. Part of the complex organization of e.g., limb movements is delegated to the spinal centers while the descending commands only specify the selection of synergies. A useful analogy is to consider that the musculo-skeletal system together with the spinal cord and brainstem can be seen as a puppet moved by strings (Loeb 2001). Pulling a single string, e.g., fixed to the hand, will move the whole arm to a new posture. And pulling just a small set of strings over time can provide a large range of movements. The descending pathways from higher parts of the brain can be seen as the implementation of these strings.

Notably the same synergy with different delay and amplitude profiles in relation with other participating synergies can be part of different locomotor modes. The influence of sensory feedback could range from minor modulatory effects on internally generated programs to extensive shaping of the spinal output in which case the final behavioral repertoire would be emergent from the complex interplay between the CNS, the body and the environment. However, data from deafferented frogs shows that 4 out of 5 previously determined synergies for the same locomotor mode persisted (Cheung et al. 2005). In order to answer the question to which extent synergies are generated internally or shaped by sensory feedback, further research is needed.

5 Conclusions

This article has presented our contributions to the current understanding of the salamander locomotor apparatus, including body kinematics, sensory feedback, internally generated activity patterns, and supraspinal control. A thorough review of the biological aspects can be found elsewhere (Cabelguen et al. 2010; Ryczko et al. 2010b). Here, we focused on the modeling aspect of this research.

In order to understand locomotion control, one requires a comprehensive and interdisciplinary approach. Locomotion is a complex dynamic phenomenon that implies the interaction between the central and peripheral nervous systems, the musculo-skeletal system, and the environment. It is very unlikely that locomotion control will be properly understood by studying specific components in isolation. Undoubtedly studies on the specific biological components are needed (e.g., motoneuron properties, muscle properties, network topology, etc.), but additionally mathematical and numerical models are essential to understand the complex interactions between these components at the system level.

A prime example for the interplay of neurophysiological experiments and modeling can be found in Ijspeert et al.

(2007). There we have built an abstract model of the spinal CPG of the salamander, on the basis of the theory of coupled oscillators. Our model suggested that limb oscillators had a slower frequency than axial oscillators. This prediction has been verified by biological experiments. We have observed in vitro that when activating limb networks and axial networks with the same pharmacological drive, the limb networks exhibited a rhythmic activity with lower frequency. The assumption that the axial network is constituted of a double chain of oscillators was demonstrated subsequently not only for the trunk network (Ryczko et al. 2010a), but also for the tail network (Charrier and Cabelguen 2011). The latter work led the hypothesis that the tail networks form an independent substructure that can be used as a "fifth limb" for additional support on some unstable substrates (e.g., on slippery surfaces). These biologically testable hypotheses were clearly guided by the architecture of the model.

Moreover extending the researcher's toolbox through the use of robots allows for the study of aspects which require a physical body for verification, e.g., body kinematics and dynamics. It allows us to test mechanisms of locomotor control with a controlled set of degrees of freedom, and thus constitute an interface between models and the real world. This is of particular importance as the physics of interaction forces in water and on solid surfaces are particularly difficult to model.

An additional illustration of the importance of the interplay between modeling and neurobiology experiments can be found in the study of Bicanski et al. (2012). The design of the model was constrained by the electrophysiological work presented in Ryczko et al. (2010a). It provided a theoretical response to the neurobiological hypothesis that a modified lamprey network can serve as a building block for the axial salamander network, and yielded a series of additional biological testable hypotheses.

A crucial ingredient is the use of models at different levels of abstraction. The choice of model is guided by the particular question investigated. To understand the cellular basis of rhythmogenesis in the locomotor network, or to account for pharmacological data, a network built at the cellular level using Hodgkin-Huxley model cells is warranted. Such models allow for the study of complex dynamics generated by a single type of conductance or the influence of a specific type of synaptic connection on the activity pattern of a single spinal segment. Oscillator models are especially suited for studies of the effects of different network topologies on e.g., intersegmental phase lag generation. In addition they lend themselves particularly well to robotic studies since they comply better with hardware constraints of the robots (e.g., onboard calculation, communication). However it remains to be determined whether the axial CPGs are composed of discrete segmental oscillators rather than distributed, overlapping modules. In salamanders CPG neurons are expected to

project to neurons that are located several segments away, as observed in other vertebrates. Consequently, although single spinal segments and hemisegments of the salamander trunk can oscillate when stimulated (Ryczko et al. 2010a), discrete oscillator models are only a first approximation, which reflects the segmental bundling of the motoneuron axons in ventral roots. Furthermore, these oscillator models need to be validated by more detailed neural network models. The models by Harishandra et al. (2011) or Bicanski et al. (2011, 2012) constitute examples and will be expanded upon in the near future. Thus, beyond an interplay of experiment and computational models, relating various models to each other must also be part of a comprehensive approach.

So far, some predictions from even our most abstract modeling studies found some resonance in physiological studies that followed them. Taken together all our studies at various levels of abstraction suggest that some common principles in axial CPG design may have been conserved through evolution. Nevertheless many points still need to be elucidated. First, the segmental circuits still need to be properly defined, in particular the type and number of interneurons involved as well as their interconnections and e.g., their susceptibility to neuromodulators. Second, the influences of different sensory inputs (e.g., cutaneous, proprioceptive, olfactory, lateral-line) need to be explored. Third, the roles of other supraspinal structures (e.g., the basal ganglia) in locomotor gait selection need to be explored. Fourth, the effect of various types of muscles on the generation of mechanical waves needs to be investigated in more detail. Finally, further work is needed, in particular in terms of modeling, to decode the interplay between spinal circuits and various descending pathways and the generation of the rich motor skills exhibited by the animal. Closing the loop between the central nervous system, sensory feedback, body mechanics and the environment via a robotic agent constitutes a unique opportunity in this undertaking.

References

Ashley-Ross MA (1994a) Hindlimb kinematics during terrestrial locomotion in salamander (*Dicamptodon tenebrosus*). J Exp Biol 193:255–283

Ashley-Ross MA (1994b) Metamorphic and speed effects on hindlimb kinematics during terrestrial locomotion in the salamander *Dicamptodon tenebrosus*. J Exp Biol 193:285–305

Ashley-Ross MA (1995) Patterns of hind limb motor output during walking in the salamander *Dicamptodon tenebrosus*, with comparisons to other tetrapods. J Comp Physiol [A] 177:273–285

Ashley-Ross MA, Lauder GV (1997) Motor patterns and kinematics during backward walking in the pacific giant salamander: evidence for novel motor output. J Neurophysiol 78:3047–3060

Ashley-Ross MA, Bechtel BF (2004) Kinematics of the transition between aquatic and terrestrial locomotion in the newt *Taricha torosa*. J Exp Biol 207:461–474

Ashley-Ross MA, Lundin R, Johnson KL (2009) Kinematics of level terrestrial and underwater walking in the California newt, *Taricha torosa*. J Exp Zool A Ecol Genet Physiol 311:240–257

Azizi E, Horton JM (2004) Patterns of axial and appendicular movements during aquatic walking in the salamander *Siren lacertina*. Zoology 107:111–120

Bar-Gad I, Kagan I (1999) Behavior of hindbrain neurons during the transition from rest to evoked locomotion in a newt. Prog Brain Res 123:285–294

Bem T, Cabelguen J-M, Ekeberg Ö, Grillner S (2003) From swimming to walking: a single basic network for two different behaviors. Biol Cybern 88:79–90

Bennett WO, Simons RS, Brainerd EL (2001) Twisting and bending: the functional role of salamander lateral hypaxial musculature during locomotion. J Exp Biol 204:1979–1989

Bicanski A, Ryczko D, Cabelguen JM, Ijspeert AJ (2011) Modeling axial spinal segments of the salamander central pattern generator for locomotion. BMC Neurosci 12(Suppl. 1):P157

Bicanski A, Ryczko D, Cabelguen JM, Ijspeert A (2012) From Lamprey to Salamander: an exploratory modeling study on the architecture of the spinal locomotor networks in the salamander. Biol Cybern. doi:10.1007/s00422-012-0538-y

Bizzi E, Tresch M, Saltiel P (2000) New perspectives on spinal motor systems. Nat Rev Neurosci 1:101–108

Bizzi E, Cheung VCK, d'Avella A, Saltiel P, Tresch M (2008) Combining modules for movement. Brain Res Rev 57:125–133

Bowtell G, Williams T (1991) Anguiliform body dynamics: modelling the interaction between muscle activation and body curvature. Phil Trans R Soc Lond B 334:385–390

Brändle K, Székely G (1973) The control of alternating coordination of limb pairs in the newt (*Triturus vulgaris*). Brain Behav Evol 8: 366–385

Buchanan JT, Grillner S, Cullheim S, Risling M (1989) Identification of excitatory interneurons contributing to generation of locomotion in lamprey: structure, pharmacology, and function. J Neurophysiol 62:59–69

Buchanan JT (2001) Contributions of identifiable neurons and neuron classes to lamprey vertebrate neurobiology. Prog Neurobiol 63: 441–466

Cabelguen J-M, Bourcier-Lucas C, Dubuc R (2003) Bimodal locomotion elicited by electrical stimulation of the midbrain in the salamander *Notophthalmus viridescens*. J Neurosci 23:2434–2439

Cabelguen J-M, Ijspeert A, Lamarque S, Ryczko D (2010) Axial dynamics during locomotion in vertebrates: lesson from the salamander. Prog Brain Res 187:149–162

Cangiano L, Grillner S (2003) Fast and slow locomotor burst generation in the hemispinal cord of the lamprey. J Neurophysiol 89:2931–2942

Carrier DR (1993) Action of the hypaxial muscles during walking and swimming in the salamander *Dicamptodon ensatus*. J Exp Biol 180:75–83

Charrier V, Lamarque S, Ryczko D, Cabelguen J-M (2010) Kinematic and electromyographical analysis of the adaptation of locomotor movements in the salamander, *Pleurodeles waltlii*. 7th Forum of European Neuroscience, Amsterdam

Charrier V, Cabelguen JM (2011) Fictive rhythmic motor patterns generated in tail segments of the adult salamander. Society for Neuroscience, Program 386.04, Abstr. TT15

Chevallier S, Jan Ijspeert A (2008) Organisation of the spinal central pattern generators for locomotion in the salamander: biology and modelling. Brain Res Rev 57:147–161

Chevallier S, Landry M, Nagy F, Cabelguen J-M (2004) Recovery of bimodal locomotion in the spinal-transected salamander, *Pleurodeles waltlii*. Eur J Neurosci 20:1995–2007

Cheng J, Stein RB, Jovanovic K, Yoshida K, Bennett DJ, Han Y (1998) Identification, localization, and modulation of neural networks for walking in the mudpuppy (*Necturus maculatus*) spinal cord. J Neurosci 18:4295–4304

Cheng J, Jovanovic K, Aoyagi Y, Bennett DJ, Han Y, Stein RB (2002) Differential distribution of interneurons in the neural networks that control walking in the mudpuppy (*Necturus maculatus*) spinal cord. Exp Brain Res 145:190–198

Cheung VC, d'Avella A, Tresch MC, Bizzi E (2005) Central and sensory contributions to the activation and organization of muscle synergies during natural motor behaviors. J Neurosci 25: 6419–6434

Cohen AH, Rossignol S, Grillner S (1988) Neural control of rhythmic movements in vertebrates. Wiley-Interscience

Cohen AH, Ermentrout GB, Kiemel T, Kopell N, Sigvardt KA, Williams TL (1992) Modelling of intersegmental coordination in the lamprey central pattern generator for locomotion. Trends Neurosci 15: 434–438

Currie SN, Stein PS (1990) Cutaneous stimulation evokes long-lasting excitation of spinal interneurons in the turtle. J Neurophysiol 64: 1134–1148

Daan S, Belterman T (1968) Lateral bending in locomotion of some lower tetrapods. Proc Ned Akad Wetten C 71:245–266

D'Août K, Aerts P, DeVree F (1996) The timing of muscle strain and activation during steady swimming in a salamander, *Ambystoma mexicanum*. Neth J Zool 46:263–271

D'Avella A, Bizzi E (1998) Low dimensionality of supraspinally induced force fields. Proc Natl Acad Sci USA 95:7711–7714

Deban SM, Schilling N (2009) Activity of trunk muscles during aquatic and terrestrial locomotion in *Ambystoma maculatum*. J Exp Biol 212:2949–2959

Deliagina TG, Zelenin PV, Fagerstedt P, Grillner S, Orlovsky GN (2000) Activity of reticulospinal neurons during locomotion in the freely behaving lamprey. J Neurophysiol 83:853–863

Delvolvé I, Bem T, Cabelguen JM (1997) Epaxial and limb muscle activity during swimming and terrestrial stepping in the adult newt, *Pleurodeles waltlii*. J Neurophysiol 78:638–650

Delvolvé I, Branchereau P, Dubuc R, Cabelguen JM (1999) Fictive rhythmic motor patterns induced by NMDA in an in vitro brain stem-spinal cord preparation from an adult urodele. J Neurophysiol 82:1074–1077

Dominici N, Ivanenko Y, Cappellini G, d'Avella A (2011) Locomotor primitives in newborn babies and their development. Science 334:997–999

Dubuc R (2009) Locomotor regions in the midbrain (MLR) and diencephalon (DLR). In: Binder MD, Hirokawa N, Windhorst U (eds) Encyclopedia of neuroscience. Springer, Berlin

Dubuc R, Brocard F, Antri M, Fénelon K, Gariépy J-F, Smetana R, Ménard A (2008) Initiation of locomotion in lampreys. Brain Res Rev 57:172–182

Edwards JL (1977) The evolution of terrestrial locomotion. In: Hecht MK, Goody PC, Hecht BM (eds) Major patterns in vertebrate evolution. Plenum Publishing Corp, New York, pp 553–576

Eidelberg E, Walden JG, Nguyen LH (1981) Locomotor control in macaque monkeys. Brain 104:647–663

Ekeberg Ö (1993) A combined neuronal and mechanical model of fish swimming. Biol Cybern 69:363–374

El Manira A, Tegnér J, Grillner S (1994) Calcium-dependent potassium channels play a critical role for burst termination in the locomotor network in lamprey. J Neurophysiol 72:1852–1861

Fagerstedt P, Orlovsky GN, Deliagina TG, Grillner S, Ullén F (2001) Lateral turns in the lamprey. II. Activity of reticulospinal neurons during the generation of fictive turns. J Neurophysiol 86:2257–2265

Frolich L, Biewener A (1992) Kinematic and electromyographic analysis of the functional role of the body axis during terrestrial and aquatic locomotion in the salamander *Ambystoma tigrinum*. J Exp Biol 162:107–130

Gillis G (1997) Anguilliform locomotion in an elongate salamander (*Siren intermedia*): effects of speed on axial undulatory movements. J Exp Biol 200:767–784

Giszter SF, Mussa-Ivaldi FA, Bizzi E (1993) Convergent force fields organized in the frog's spinal cord. J Neurosci 13:467–491

Grillner S (1981) Control of locomotion in bipeds, tetrapods, and fish. In: Brooks VB (ed) Handbook of physiology, the nervous system. Motor control. Bethesda, Am Physiol Soc, sect. I, vol 2, pp 1179–1236

Grillner S, McClellan A, Sigvardt K (1982) Mechanosensitive neurons in the spinal cord of the lamprey. Brain Res 235:169–173

Grillner S, Williams T, Lagerback PA (1984) The edge cell, a possible intraspinal mechanoreceptor. Science 223:500–503

Grillner S, Wallén P (1985) Central pattern generators for locomotion, with special reference to vertebrates. Annu Rev Neurosci 8:linebreak 233–261

Grillner S, Georgopoulos AP, Jordan LM (1997) Selection and initiation of motor behavior. In: Stein PSG, Grillner S, Selverston AI, Stuart DG (eds) Neurons, networks, and motor behavior. MIT Press, Cambridge, pp. 3–19

Grillner S (2006) Biological pattern generation: the cellular and computational logic of networks in motion. Neuron 52:751–766

Grillner S (2011) Human locomotor circuits conform. Science 334: 912–913

Guan L, Kiemel T, Cohen AH (2001) Impact of movement and movement-related feedback on the lamprey central pattern generator for locomotion. J Experim Biol 204:2361–2370

Hagevik A, McClellan AD (1994) Coupling of spinal locomotor networks in larval lamprey revealed by receptor blockers for inhibitory amino acids: neurophysiology and computer modeling. J Neurophysiol 72:1810–1829

Harper CE, Roberts A (1993) Spinal cord neuron classes in embryos of the smooth newt *Triturus vulgaris*: a horseradish peroxidase and immunocytochemical study. Philos Trans R Soc Lond B Biol Sci 340:141–160

Harishandra N, Cabelguen JM, Ekeberg O (2010) A 3D Musculomechanical model of the salamander for the study of different gaits and modes of locomotion. Front Neurorobot 4:112

Harischandra N, Knuesel J, Kozlov A, Bicanski A, Cabelguen JM, Ijspeert AJ, Ekeberg Ö (2011) Sensory feedback plays a significant role in generating walking gait and in gait transition in salamanders: a simulation study. Front Neurorobot 5:3

Hill AAV, Masino MA, Calabrese RL (2003) Intersegmental coordination of rhythmic motor patterns. J Neurophysiol 90:531–538

Hubbard CS, Dolence EK, Rose JD (2010) Brainstem reticulospinal neurons are targets for corticotropin-releasing factor-Induced locomotion in roughskin newts. Horm Behav 57:237–246

Ijspeert AJ (2001) A connectionist central pattern generator for the aquatic and terrestrial gaits of a simulated salamander. Biol Cybern 84:331–348

Ijspeert AJ, Crespi A, Cabelguen J-M (2005) Simulation and robotics studies of salamander locomotion: applying neurobiological principles to the control of locomotion in robots. Neuroinf 3:171–195

Ijspeert AJ, Crespi A, Ryczko D, Cabelguen J-M (2007) From swimming to walking with a salamander robot driven by a spinal cord model. Science 315:1416–1420

Ijspeert AJ (2008) Central pattern generators for locomotion control in animals and robots: a review. Neural Netw 21:642–653

Jackson AW, Horinek DF, Boyd MR, McClellan AD (2005) Disruption of left-right reciprocal coupling in the spinal cord of larval lamprey abolishes brain-initiated locomotor activity. J Neurophysiol 94:2031–2044

Jacobson R, Hollyday MA (1982) Electrically evoked walking and fictive locomotion in the chick. J Neurophysiol 48:257–270

Jovanovic K, Burke RE (2004) Morphology of brachial segments in mudpuppy (*Necturus maculosus*) spinal cord studied with confocal and electron microscopy. J Comp Neurol 471:361–385

Jovanovic K, Petrov T, Stein RB (1999) Effects of inhibitory neurotransmitters on the mudpuppy (*Necturus maculatus*) locomotor pattern in vitro. Exp Brain Res 129:172–184

Karakasiliotis K, Schilling N, Cabelguen JM, Ijspeert AJ (2012) How far are we in understanding salamander's locomotion: a kinematics perspective from biology and robotics. Biol Cybern (submitted to—same issue)

Kiemel T, Cohen AH (2001) Bending the lamprey spinal cord causes a slowly-decaying increase in the frequency of fictive swimming. Brain Res 900:57–64

Knuesel J, Ijspeert AJ (2011) Effects of muscle dynamics and proprioceptive feedback on the kinematics and CPG activity of salamander stepping. BMC Neurosci 12(Suppl. 1):P157

Kopell N, Ermentrout GB, Williams TL (1991) On chains of oscillators forced at one end. SIAM J Appl Math 51:1397–1417

Kozlov A, Huss M, Lansner A, Kotaleski JH, Grillner S (2009) Simple cellular and network control principles govern complex patterns of motor behavior. Proc Natl Acad Sci USA 106:20027–20032

Kozlov A, Lansner A, Grillner S, Kotaleski JH (2007) A hemicord locomotor network of excitatory interneurons: a simulation study. Biol Cybern 96(2):229–243

Lamarque S, Ryczko D, Didier H, Cabelguen J-M (2009) Dynamics of the axial locomotor network in intact, freely moving salamanders. Neural Chall. 31st International symposium of GRSNC, Montréal

Lavrov I, Cheng J (2004) Activation of NMDA receptors is required for the initiation and maintenance of walking-like activity in the mudpuppy (*Necturus maculatus*). Can J Physiol Pharmacol 82:637–644.

Lavrov I, Cheng J (2008) Methodological optimization of applying neuroactive agents for the study of locomotor-like activity in the mudpuppies (*Necturus maculatus*). J Neurosci Methods 174:97–102

Le Ray D, Juvin L, Ryczko D (2011) Supraspinal control of locomotion: the mesencephalic locomotor region. Prog Brain Res 188:51–70

Lemon RN (2008) Descending pathways in motor control. Annu Rev Neurosci 31:195–218

Loeb G (2001) Learning from the spinal cord. J Physiol 533:111–117

Lowry CA, Rose JD, Moore FL (1996) Corticotropin-releasing factor enhances locomotion and medullary neuronal firing in an amphibian. Horm Behav 30:50–59

Matsushima T, Grillner S (1992) Neural mechanisms of intersegmental coordination in lamprey: local excitability changes modify the phase coupling along the spinal cord. J Neurophysiol 67:373–388

McClellan AD (1986) Command systems for initiating locomotor responses in fish and amphibians—parallels to initiation of locomotion in mammals. In: Grillner S, Stein P, Stuart D, Forssberg H, Herman R (eds) Neurobiology of vertebrate locomotion, Wenner-Gren symposium series. MacMillan Press, London, vol 45, pp. 3–20.

McCrea DA, Rybak IA (2008) Organization of mammalian locomotor rhythm and pattern generation. Brain Res Rev 57:134–146

Muller E, Buessing L, Schemmel J, Meier K (2007) Spike-frequency adapting neural ensembles: beyond mean adaptation and renewal theories. Neural Comput 19:2958–3010

Mullins OJ, Hackett JT, Buchanan JT, Friesen OW (2011) Neuronal control of swimming behavior: comparison of vertebrate and invertebrate model system. Prog Neurobiol 93:244–269

Mussa-Ivaldi FA, Giszter SF, Bizzi E (1994) Linear combinations of primitives in vertebrate motor control. Proc Natl Acad Sci USA 91:7534–7538

Pearson KG (1993) Common principles of motor control in vertebrates and invertebrates. Annu Rev Neurosci 16:265–297

Pearson K, Ekeberg Ö, Büschges A (2006) Assessing sensory function in locomotor systems using neuro-mechanical simulations. Trends Neurosci 29:625–631

Peters SE, Goslow GE Jr (1983) From salamanders to mammals: continuity in musculoskeletal function during locomotion. Brain Behav Evol 22:191–197

Rauscent A (2008) Remaniements fonctionnels des réseaux locomoteurs spinaux au cours du développement de l'amphibien Xenopus laevis en métamorphose. PhD thesis, Université Bordeaux 1, Bordeaux

Roos P (1964) Lateral bending in newt locomotion. Proc Ned Akad Wetten C 67:223–232

Rossignol S, Chau C, Brustein E, Giroux N, Bouyer L, Barbeau H, Reader TA (1998) Pharmacological activation and modulation of the central pattern generator for locomotion in the cat. Ann N Y Acad Sci 860:346–359

Rossignol S, Dubuc R, Gossard JP (2006) Dynamic sensorimotor interactions in locomotion. Physiol Rev 86:89–154

Ryczko D (2008) Dynamique de l'organisation fonctionnelle des réseaux locomoteurs chez la salamandre: du module rythmogène à une palette de modes locomoteurs. PhD thesis, Université de Bordeaux 2, Bordeaux

Ryczko D, Lamarque S, Didier H, Cabelguen JM (2009) Dynamics of the axial locomotor network in the isolated spinal cord of the salamander. Society for Neuroscience, Program 565.8, Abstr. EE6

Ryczko D, Charrier V, Ijspeert A, Cabelguen JM (2010a) Segmental oscillators in axial motor circuits of the salamander: distribution and bursting mechanisms. J Neurophysiol 104:2677–2692

Ryczko D, Dubuc R, Cabelguen J-M (2010b) Rhythmogenesis in axial locomotor networks: an interspecies comparison. Prog Brain Res 187:189–211

Saltiel P, Tresch MC, Bizzi E (1998) Spinal cord modular organization and rhythm generation: an NMDA iontophoretic study in the frog. J Neurophysiol 80:2323–2339

Schroeder DM, Egar MW (1990) Marginal neurons in the urodele spinal cord and the associated denticulate ligaments. J Comp Neurol 301:93–103

Shik ML, Severin FV, Orlovskii GN (1966) Control of walking and running by means of electric stimulation of the midbrain. Biofizika 11:659–666

Skinner RD, Garcia-Rill E (1984) The mesencephalic locomotor region (MLR) in the rat. Brain Res 323:385–389

Steeves JD, Sholomenko GN, Webster DMS (1987) Stimulation of the pontomedullary reticular formation initiates locomotion in decerebrate birds. Brain Res 401:205–212

Székely G, Czéh G (1976) Organisation of Locomotion. In: Llinás RR, Precht W, Capranica RR (eds) Frog neurobiology: a handbook, Springer Verlag, Berlin, pp. 765–792

Székely G, Czéh G, Vörös G (1969) The activity pattern of limb muscles in freely moving normal and deafferented newts. Exp Brain Res 9:53–72

Tresch MC, Bizzi E (1999) Responses to spinal microstimulation in the chronically spinalized rat and their relationship to spinal systems activiated by low threshold cutaneous stimulation. Exp Brain Res 129:401–416

Tresch MC, Kiehn O (2002) Synchronization of motor neurons during locomotion in the neonatal rat: predictors and mechanisms. J Neurosci 22:9997–10008

Tytell E, Hsu C, Williams T, Cohen AH, Fauci LJ (2010) Interactions between internal forces, body stiffness, and fluid environment in a

neuromechanical model of lamprey swimming. Proc Natl Acad Sci USA 107:19832–19837

Uematsu K, Todo T (1997) Identification of the midbrain locomotor nuclei and their descending pathways in the teleost carp. Cyprinus carpio Brain Res 773:1–7

van den Kieboom J (2009) Biped locomotion and stability—a practical approach. Masters thesis, Department of Artificial Intelligence, University of Groningen, the Netherlands

Wallén P, Williams TL (1984) Fictive locomotion in the lamprey spinal cord in vitro compared with swimming in the intact and spinal animal. J Physiol 347:225–239

Wallén P, Grillner S (1997) Central pattern generators and their interaction with sensory feedback. Proc Am Control Conf 5:2851–2855

Wallén P, Ekeberg O, Lansner A, Brodin L, Tråvén H, Grillner S (1992) A computer-based model for realistic simulations of neural networks. II. The segmental network generating locomotor rhythmicity in the lamprey. J Neurophysiol 68:1939–1950

Wheatley M, Edamura M, Stein RB (1992) A comparison of intact and in vitro locomotion in an adult amphibian. Exp Brain Res 88:609–614

Wheatley M, Jovanovic K, Stein RB, Lawson V (1994) The activity of interneurons during locomotion in the in vitro necturus spinal cord. J Neurophysiol 71:2025–2032

Wheatley M, Stein RB (1992) An in vitro preparation of the mudpuppy for simultaneous intracellular and electromyographic recording during locomotion. J Neurosci Methods 42:129–137

Williams TL, Sigvardt KA, Kopell N, Ermentrout GB, Remler MP (1990) Forcing of coupled nonlinear oscillators: studies of intersegmental coordination in the lamprey locomotor central pattern generator. J Neurophysiol 64:862–871